Dyes and Pigments 104 (2014) 8–14

Contents lists available at ScienceDirect

Dyes and Pigments

journal homepage: www.elsevier.com/locate/dyepig

Influence of different substituents linked on fluorene spacer in organic sensitizers on photovoltaic properties

Zhenhua Ci, Xiaoqiang Yu*, Chaolei Wang, Tingli Ma, Ming Bao*

State Key Laboratory of Fine Chemicals, Dalian University of Technology, Dalian 116023, China

ARTICLE INFO

Article history:
Received 19 November 2013
Received in revised form
17 December 2013
Accepted 20 December 2013
Available online 31 December 2013

Keywords:
Dye-sensitized solar cells
Organic dye
n-Hexyl group
Fluorene
π-Conjugated system
Photon-to-current conversion efficiency

ABSTRACT

New metal-free organic sensitizers containing a fluorene unit as a π-conjugated system, a diphenylamine as an electron donor, and a cyanoacrylic acid moiety as an electron acceptor were synthesized and used for dye-sensitized solar cells. The photophysical and electrochemical properties of these dyes were investigated, and their performances as sensitizers in solar cells were measured. One solar cell containing the *n*-hexyl group in the fluorene unit produced an η of 5.15% (J_{sc} = 9.69 mA cm^{-2}, V_{oc} = 0.77 V, and ff = 0.70) under 100 mW cm^{-2} simulated AM 1.5 G solar irradiation (100 mW cm^{-2}).

1. Introduction

Dye-sensitized solar cells (DSSCs) have attracted significant attention in recent years because of their high efficiency, low cost, and facile fabrication [1–3]. DSSCs based on Ru(II)-polypyridyl complex photosensitizers, such as N3, N719, and the black dye, have achieved remarkable conversion efficiency of up to 11% under AM 1.5 irradiation conditions [4–6]. However, the main drawbacks of the Ru(II) complex sensitizers include the cost of ruthenium metal, the requirement for cautious synthesis, and the tedious purification process. Metal-free organic dyes have gained increasing attention because of their unique advantages, such as high molar absorption coefficient, ease of structure modification, and relatively low material cost [7–10].

A common organic dye for DSSCs contains a structure of electron donor/acceptor (D–A) that is linked through a π-conjugated bridge; this structure is called the D–π–A molecular structure [11]. In this structure, triphenylamine derivatives have been widely used as the electron donor (D), whereas a cyanoacrylic acid moiety acts as the electron acceptor (A). D–π–A dyes based on triphenylamine moieties with various π-conjugated bridges, such as benzene [12–18], thiophene [19–22], thienothiophene [23–27], dithienothiophene [28,29], benzo[*b*]thiophene [30,31], benzothiadiazole [32–35], or dibenzosilole [36] have been designed and synthesized as efficient sensitizers to achieve high conversion efficiency in DSSC devices. The π-conjugated bridge has a great influence on the photoelectronic properties of D–π–A dyes. Generally, some steric structures should be introduced to the π-conjugated bridge to inhibit unfavorable π–π aggregation [37]. However, the influence of different substituted groups on the π-conjugated bridge to avoid π–π aggregation has not been systematically studied.

This study presents three new organic dyes (**F1**, **F2**, and **F3**) with different group-substituted fluorene moieties as π-conjugated bridge, a diphenylamine moiety as electron donor, and a cyanoacetic acid as electron acceptor (Fig. 1). The study also investigates the photophysical, electrochemical, and photovoltaic properties.

2. Experimental section

2.1. General analytical measurements

All chemicals were used as received from commercial sources without purification. Solvents for chemical synthesis, such as dichloromethane, dimethylformamide, toluene, and tetrahydrofuran, were purified by distillation. 2,7-Dibromo-9,9-diphenyl-9H-fluorene [38] and 2,7-dibromo-9,9-dihexyl-9H-fluorene [39] were synthesized according to the reported literature. ^{1}H and ^{13}C NMR spectra were recorded on either Varian Inova-400 spectrometer

* Corresponding authors. Tel.: +86 411 84986181; fax: +86 411 84986180.
E-mail address: yuxiaoqiang@dlut.edu.cn (X. Yu).

0143-7208/$ – see front matter © 2013 Elsevier Ltd. All rights reserved.
http://dx.doi.org/10.1016/j.dyepig.2013.12.020

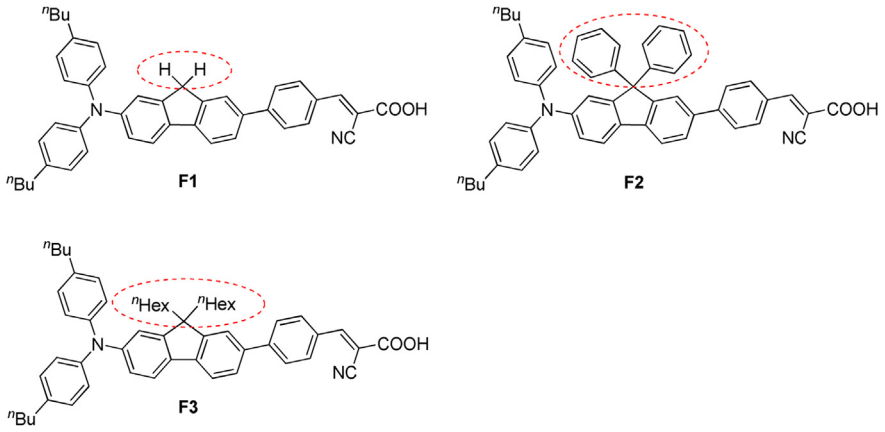

Fig. 1. Molecular structures of dyes **F1, F2,** and **F3**.

(400 MHz for ^{1}H; 100 MHz for ^{13}C) or Bruker Avance II-400 spectrometer (400 MHz for ^{1}H; 100 MHz for ^{13}C); $CDCl_3$ and TMS were used as solvent and internal standard, respectively. High-resolution mass spectra were recorded on either Q-TOF or GC-TOF mass spectrometer.

2.2. Theoretical calculations

Gaussian 03 package was used for density functional theory calculation [40]. The geometries and energies of **F1**, **F2**, and **F3** were determined using the B3LYP method with the 6-31G (d) basis set.

2.3. Synthesis

The synthetic routes to the **F1**, **F2**, and **F3** dyes are shown in Scheme 1.

2.3.1. Synthesis of 7-bromo-N,N-bis(4-butylphenyl)-9H-fluoren-2-amine (*4*)

A mixture of bis(4-butylphenyl)amine (1.407 g, 5 mmol), 2,7-dibromo-9H-fluorene **1** (3.2401 g, 10 mmol), sodium *tert*-butoxide (0.961 g, 10 mmol), dppf (0.0641 g, 0.12 mmol), $Pd(dba)_2$ (0.0575 g, 0.1 mmol), and toluene (80 ml) was refluxed under nitrogen atmosphere for 24 h. After cooling to room temperature, water was added to quench the reaction. The product was extracted with dichloromethane (20 mL × 3). The combined organic layers were dried over anhydrous $MgSO_4$, and the solvent was removed under vacuum. The crude product was purified by column chromatography on silica (petroleum ether/ethyl acetate = 100/1, v/v) to give a colorless oil **4** (1.2212 g, 2.33 mmol, 47%). ^{1}H NMR (400 MHz, $CDCl_3$) δ 7.58–7.53 (m, 2H), 7.49 (d, J = 8.0 Hz, 1H), 7.43 (d, J = 7.8 Hz, 1H), 7.23 (s, 1H), 7.19 (s, 1H), 7.07–7.00 (m, 8H), 3.74 (s, 2H), 2.56 (t, J = 7.6 Hz, 4H), 1.61–1.56 (m, 4H), 1.40–1.34 (m, 4H), 0.94 (t, J = 7.2 Hz, 6H). ^{13}C NMR (100 MHz, $CDCl_3$) δ 147.9, 145.6, 145.0, 144.2, 140.7, 137.5, 134.7, 129.8, 129.2, 128.1, 124.4, 122.4, 120.4, 119.7, 119.3, 36.7, 35.1, 33.8, 22.5, 14.1. HRMS (EI): calcd. for $C_{33}H_{34}NBr$, 523.1875 $[M]^{+}$; found, 523.1870.

2.3.2. Synthesis of 7-bromo-N,N-bis(4-butylphenyl)-9,9-diphenyl-9H-fluoren-2-amine (*5*)

The synthetic route of **5** is similar with **4** to give a white solid in 63% yield. mp 168–169 °C. ^{1}H NMR (400 MHz, d_6-DMSO) δ 7.77 (dd, J = 8.0 Hz, 7.7 Hz, 2H), 7.55 (dd, J = 8.1 Hz, 3.4 Hz, 2H), 7.29–7.22 (m, 6H), 7.08 (d, J = 8.4 Hz, 4H), 7.02–6.84 (m, 10H), 2.56 (t, J = 7.1 Hz, 4H), 1.54–1.49 (m, 4H), 1.32–1.23 (m, 4H), 0.87 (t, J = 7.3 Hz, 6H). ^{13}C NMR (100 MHz, $CDCl_3$) δ 152.7, 152.2, 148.4, 145.3, 145.2, 139.3,

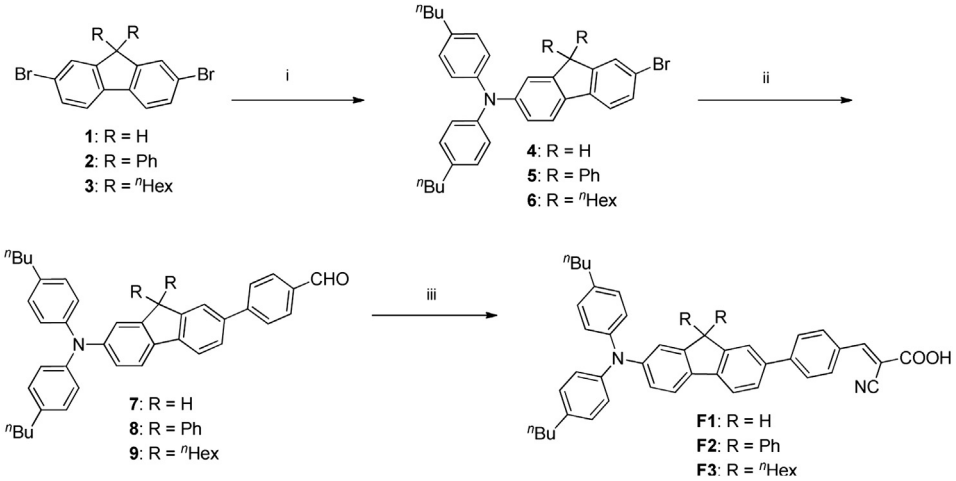

Scheme 1. The synthetic routes for **F1**, **F2** and **F3** dyes: i) bis(4-butylphenyl)amine, $Pd(dba)_2$, dppf, $^{t}BuONa$, toluene, 110 °C; ii) (4-formylphenyl)boronic acid, $Pd(PPh_3)_4$, K_2CO_3, THF, refluxed; iii) cyanoacetic acid, NH_4OAc, glacial CH_3COOH, refluxed.

137.7, 132.5, 130.7, 129.4, 129, 128.3, 128.2, 126.8, 124.4, 122.1, 120.7, 120.3, 120.0, 65.4, 35.1, 33.7, 22.5, 14.1. HRMS (EI): calcd. for $C_{45}H_{42}NBr$, 675.2501 $[M]^+$; found, 675.2494.

2.3.3. Synthesis of 7-bromo-N,N-bis(4-butylphenyl)-9,9-dihexyl-9H-fluoren-2-amine (**6**)

The synthetic route of **6** is similar with **4** to give a colorless oil in 63% yield. ^1H NMR (400 MHz, $CDCl_3$) δ 7.47 (d, $J = 8.2$ Hz, 1H), 7.44–7.38 (m, 3H), 7.06–6.96 (m, 10 H), 2.57 (t, $J = 7.8$ Hz, 4H), 1.81 (t, $J = 8.0$ Hz, 4H), 1.64–1.56 (m, 4H), 1.42–1.33 (m, 4H), 1.16–1.05 (m, 12 H), 0.96–0.91 (m, 6H), 0.81 (t, $J = 7.2$ Hz, 6H), 0.64–0.63 (m, 4H). ^{13}C NMR (100 MHz, $CDCl_3$) δ 152.9, 151.6, 148.0, 145.6, 140.1, 137.2, 136.8, 134.3, 129.8, 129.1, 129.0, 125.9, 123.9, 123.8, 122.7, 120.3, 119.9, 118.4, 55.3, 40.2, 35.1, 33.7, 31.5, 29.6, 23.7, 22.6, 22.5, 14.0. HRMS (EI): calcd. for $C_{45}H_{58}NBr$, 691.3753 $[M]^+$; found, 691.3755.

2.3.4. Synthesis of 4-(7-(bis(4-butylphenyl)amino)-9H-fluoren-2-yl)benzaldehyde (**7**)

A mixture of compound **5** (1.049 g, 2 mmol), (4-formylphenyl) boronic acid (0.4498 g, 3 mmol), $Pd(PPh_3)_4$ (0.116 g, 0.1 mmol), Na_2CO_3 (1.106 g, 8 mmol) and THF-H_2O (10 mL–2 mL) was refluxed under nitrogen atmosphere for 24 h. After cooling to room temperature, water was added to quench the reaction. The product was extracted with dichloromethane (20 mL × 3). The combined organic layers were dried over anhydrous $MgSO_4$, and the solvent was removed under vacuum. The crude product was purified by column chromatography on silica (petroleum ether/ethyl acetate = 10/1, v/v) to give a yellow solid **7** (0.9796 g, 1.782 mmol, 89%). mp 90–91 °C. ^1H NMR (400 MHz, $CDCl_3$) δ 10.00 (s, 1H), 7.93 (d, $J = 8.2$ Hz, 2H), 7.80 (d, $J = 8.2$ Hz, 2H), 7.75 (d, $J = 8.5$ Hz, 2H), 7.64–7.62 (m, 2H), 7.10–7.02 (m, 10 H), 3.85 (s, 2H), 2.58 (t, $J = 7.7$ Hz, 4H), 1.63–1.57 (m, 4H), 1.41–1.34 (m, 4H), 0.95 (t, $J = 7.3$ Hz, 6H). ^{13}C NMR (100 MHz, $CDCl_3$) δ 145.6, 145.0, 143.9, 142.3, 139.7, 137.6, 137.0, 135.2, 135.0, 134.9, 130.3, 130.2, 129.2, 129.0, 128.5, 127.7, 127.5, 127.4, 126.3, 124.5, 123.8, 122.3, 120.6, 119.7, 119.6, 37.0, 35.1, 33.7, 22.5, 14.0. HRMS (EI): calcd. for $C_{40}H_{39}NO$, 549.3032 $[M]^+$; found, 549.3039.

2.3.5. Synthesis of 4-(7-(bis(4-butylphenyl)amino)-9,9-diphenyl-9H-fluoren-2-yl)benzaldehyde (**8**)

The synthetic route of **8** is similar with **7** to give a yellow solid in 91% yield. mp 144–145 °C. ^1H NMR (400 MHz, d_6-DMSO) δ 10.02 (s, 1H), 7.94 (dd, $J = 8.1$ Hz, 10.3 Hz, 3H), 7.86 (d, $J = 8.1$ Hz, 2H), 7.82 (dd, $J = 7.8$ Hz, 7.4 Hz, 2H), 7.77 (s, 1H), 7.27–7.21 (m, 6H), 7.10–7.08 (m, 8H), 6.92–6.90 (m, 6H), 1.57–1.49 (m, 4H), 1.32–1.24 (m, 6H), 0.91–0.84 (m, 8H). ^{13}C NMR (100 MHz, $CDCl_3$) δ 191.9, 153.0, 151.7, 148.6, 147.4, 145.8, 145.2, 140.9, 137.8, 137.7, 135.0, 132.8, 130.3, 129.2, 128.4, 128.3, 127.6, 127.1, 126.8, 125.1, 124.5, 122.1, 121.0, 120.4, 120.0, 65.6, 35.2, 33.8, 31.7, 22.8, 22.5, 14.3, 14.2. HRMS (EI): calcd. for $C_{52}H_{47}NO$, 701.3658 $[M]^+$; found, 701.3666.

2.3.6. Synthesis of 4-(7-(bis(4-butylphenyl)amino)-9,9-dihexyl-9H-fluoren-2-yl)benzaldehyde (**9**)

The synthetic route of **9** is similar with **7** to give a yellow oil in 82% yield. ^1H NMR (400 MHz, $CDCl_3$) δ 10.05 (s, 1H), 7.96 (d, $J = 8.3$ Hz, 2H), 7.82 (d, $J = 8.2$ Hz, 2H), 7.66 (d, $J = 7.8$ Hz, 1H), 7.60–7.54 (m, 3H), 7.12–6.99 (m, 10H), 2.58 (t, $J = 7.6$ Hz, 4H), 1.94–1.87 (m, 4H), 1.63–1.59 (m, 4H), 1.41–1.37 (m, 4H), 1.16–1.07 (m, 12 H), 0.94 (t, $J = 7.3$ Hz, 6H), 0.801 (t, $J = 6.9$ Hz, 6H), 0.71–0.70 (m, 4H). ^{13}C NMR (100 MHz, $CDCl_3$) δ 191.9, 152.4, 151.6, 148.1, 147.8, 145.7, 141.8, 137.3, 134.9, 134.6, 130.3, 129.1, 127.6, 126.4, 124.0, 122.7, 121.4, 120.6, 119.4, 118.4, 55.2, 40.3, 35.1, 33.7, 31.6, 29.7, 23.9, 22.6, 22.5, 14.1. HRMS (EI): calcd. for $C_{52}H_{63}NO$, 717.4910 $[M]^+$; found, 717.4918.

2.3.7. Synthesis of 3-(4-(7-(bis(4-butylphenyl)amino)-9H-fluoren-2-yl)phenyl)-2-cyanoacrylic acid (***F1***)

A mixture of **7** (0.5497 g, 1 mmol), cyanoacetic acid (1.1 mmol, 0.094 g), ammonium acetate (0.25 mmol, 0.02 g), and acetic acid (5 mL) was refluxed under nitrogen atmosphere for 5 h. After cooling to room temperature, water was added to quench the reaction. The product was extracted with dichloromethane (10 mL × 3). The combined organic layers were dried over anhydrous $MgSO_4$, and the solvent was removed under vacuum. The crude product was purified by column chromatography on silica (dichloromethane/ethanol = 20/1, v/v) to give a red solid **F1** (0.4694 g, 0.761 mmol, 76%). mp 154–155 °C. ^1H NMR (400 MHz, d_6-DMSO) δ 8.06 (s, 1H), 7.99 (d, $J = 8.4$ Hz), 7.88 (d, $J = 4.2$ Hz, 2H), 7.84 (d, $J = 7.6$ Hz, 2H), 7.55 (dd, $J = 8.3$ Hz, 8.0 Hz, 2H), 7.11 (d, $J = 8.3$ Hz, 5H), 6.94 (d, $J = 8.3$ Hz, 5H), 3.86 (s, 2H), 3.01 (t, $J = 7.1$ Hz, 4H), 1.58–1.50 (m, 4H), 1.36–1.29 (m, 4H), 0.90 (t, $J = 7.3$ Hz, 6H). ^{13}C NMR (100 MHz, d_6-DMSO) δ 164.2, 148.2, 147.6, 145.6, 145.4, 144.1, 143.2, 141.6, 137.5, 136.9, 135.2, 132.1, 130.7, 129.8, 127.4, 126.2, 124.6, 123.7, 122.1, 121.5, 120.2, 119.6, 119.5, 45.7, 34.7, 33.6, 22.3, 14.3, 9.2. MS (LD, m/z): calcd. for $C_{43}H_{40}N_2O_2$, 616.3090 $[M]^+$; found, 616.2932.

2.3.8. Synthesis of 3-(4-(7-(bis(4-butylphenyl)amino)-9,9-diphenyl-9H-fluoren-2-yl)phenyl)-2- cyanoacrylic acid (***F2***)

The synthetic route of **F2** is similar with **F1** to give a red solid in 78% yield. mp 208–209 °C. ^1H NMR (400 MHz, d_6-DMSO) δ 8.05 (s, 1H), 7.97 (d, $J = 8.4$ Hz, 2H), 7.89 (d, $J = 8.0$ Hz, 1H), 7.81 (d, $J = 8.4$ Hz, 1H), 7.79–7.76 (m, 4H), 7.26–7.21 (m, 6H), 7.09–7.07 (m, 8H), 6.90 (d, $J = 8.5$ Hz, 6H), 2.52 (t, $J = 7.1$ Hz, 4H), 1.57–1.49 (m, 4H), 1.34–1.25 (m, 4H), 0.89 (t, $J = 7.3$ Hz, 6H). ^{13}C NMR (100 MHz, d_6-DMSO) δ 152.8, 151.3, 148.2, 145.7, 145.3, 144.6, 140.3, 137.5, 133.1, 131.2, 129.1, 128.2128.1, 126.6, 124.4, 122.0, 120.9, 120.6, 119.8, 65.5, 35.1, 33.7, 22.5, 14.1, 1.1. HRMS (EI): calcd. for $C_{55}H_{48}N_2O_2$, 768.3716 $[M]^+$; found, 768.3725.

2.3.9. Synthesis of 3-(4-(7-(bis(4-butylphenyl)amino)-9,9-dihexyl-9H-fluoren-2-yl)phenyl)-2- cyanoacrylic acid (***F3***)

The synthetic route of **F3** is similar with **F1** to give a red solid in 82% yield. mp 191–192 °C. ^1H NMR (400 MHz, d_6-DMSO) δ 8.32 (s, 1H), 8.08 (s, 2H), 7.80 (s, 2H), 7.69–7.48 (m, 4H), 6.98–6.83 (m, 10H), 2.55 (t, $J = 7.6$ Hz, 4H), 1.87–1.81 (m, 4H), 1.69–1.53 (m, 4H), 1.41–1.37 (m, 4H), 1.18–1.10 (m, 12 H), 0.95 (t, $J = 7.3$ Hz, 6H), 0.75 (t, $J = 6.9$ Hz, 6H), 0.64–0.62 (m, 4H). ^{13}C NMR (100 MHz, d_6-DMSO) δ 163.8, 154.0, 152.3, 151.4, 147.8, 145.5, 145.2, 141.5, 136.9, 134.8, 131.8, 130.5, 129.3, 127.4, 126.3, 123.9, 122.6, 121.3, 120.0, 118.3, 116.7, 103.2, 55.0, 34.7, 33.5, 31.3, 29.4, 23.8, 22.4, 22.2, 14.1. HRMS (EI): calcd. for $C_{55}H_{64}N_2O_2$, 784.4968$[M]^+$; found, 784.4977.

2.4. Fabrication of DSSCs

The screen-printable TiO_2 pastes were prepared according to the procedure developed by Ma's group [41]. A screen-printing technique was used to fabricate TiO_2 films. First, the paste was deposited on a fluorine-doped tin oxide (FTO) conductive glass (Asahi Glass Co., Ltd.; sheet resistance, 10 Ω/sq). Second, the film was sintered at 450 °C for 30 min in atmospheric air, immersed in 40 mM $TiCl_4$ solution for 30 min at 70 °C, rinsed with water and ethanol, and sintered at 500 °C for 30 min. The film was dipped into **F1**, **F2**, and **F3** dye solutions (0.4 mM in CH_2Cl_2) for 18 h after cooling to 80 °C. Finally, dye-sensitized TiO_2 photoelectrodes (thickness, 12 μm) were obtained. The organic electrolyte was composed of 0.06 M LiI, 0.03 M I_2, 0.1 M guanidinium thiocyanate, 0.6 M 1-propyl-3-methylimidazolium iodide (PMII), and 0.5 M *tert*-butyl-pyridine in acetonitrile. The active area of DSSCs was 0.16 cm^2. DSSC devices were assembled with counter electrodes

(thermally platinized FTO) using a thermoplastic frame (Surlyn, 60 μm thick).

2.5. Measurements

Absorption and emission spectra were recorded with HP8453 (USA) and PTI700 (USA), respectively. Electrochemical measurement was carried out on a BAS100W (USA) electrochemistry workstation. The irradiation source for the photocurrent–voltage measurement was an AM 1.5 solar simulator (16S-002, Solar Light Co. Ltd., USA). The incident light intensity was 100 mW cm^{-2} calibrated with a standard silicon solar cell. The current–voltage curve was obtained by linear sweep voltammetry method using an electrochemical workstation (LK9805, Lanlike Co. Ltd., China). The incident photon-to-current conversion efficiency (IPCE) measurement was performed by a Hypermonolight (SM-25, Jasco Co. Ltd., Japan).

3. Results and discussion

3.1. Synthesis

The organic dyes **F1**, **F2**, and **F3** were synthesized following the steps depicted in Scheme 1. Compounds of **4**–**6** were prepared via the Buchwald–Hartwig cross-coupling reaction of bis(4-butylphenyl)amine with the corresponding dibromo compounds. Coupling reactions of **4**–**6** with 4-formyl phenyl boronic acid under the Suzuki reaction led to their corresponding aldehydes **7**–**9**. Finally, the aldehydes were condensed with cyanoacetic acid to obtain the target compounds **F1**, **F2**, and **F3** via Knöevenagel reaction in the presence of ammonium acetate.

3.2. Absorption properties in solution

The optical and electrochemical properties of the three dyes are summarized in Fig. 2 and Table 1. Fig. 2 shows that all dyes in CH_2Cl_2 solutions gave two distinct absorption bands: one relatively weak band in the near-ultraviolet region (300 nm–320 nm) that corresponds to the π–π* electron transition and another with a strong absorption in the visible region (420 nm–460 nm). The bands can be assigned to an intramolecular charge transfer between the triarylamine donating unit and the cyanoacrylic acid anchoring moiety, thereby producing an efficient charge-separated state.

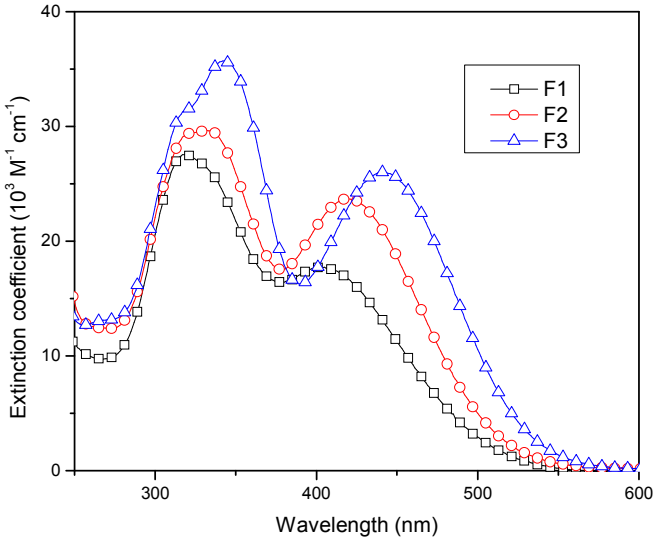

Fig. 2. Absorption spectra of **F1, F2,** and **F3** in CH_2Cl_2 at ambient temperature.

Table 1
Optical and electrochemical properties of **F1**, **F2**, and **F3** dyes.

Dye	Absorption[a]		Emission[a]	Oxidation potential		
	λ_{max} [nm]	ε at λ_{max} [M^{-1} cm^{-1}]	λ_{max} [nm]	E_{ox}[V][b] (versus NHE)	E_{0-0} [V][c] (Abs/Em)	ELUMO[V] (versus NHE)
F1	405	17,732	645	0.95	2.46	−1.51
F2	418	23,695	636	0.97	2.38	−1.41
F3	441	26,016	623	0.93	2.41	−1.48

[a] Absorption and emission spectra were measured in CH_2Cl_2, with a concentration of 1.0×10^{-5} M at room temperature.
[b] The oxidation potential of the dyes was measured under the following conditions: working electrode, Pt; electrolyte, 0.1 M tetrabutylammonium hexafluorophosphate, *n*-Bu_4NPF_6 in THF; scan rate, 0.1 V/s. Potentials measured vs Fe^+/Fe were converted to NHE by addition of +0.63 V.
[c] The E_{0-0} energies were estimated from the intercept of the normalized absorption and emission spectra.

Compared with **F1** (405 nm, 17,732 M^{-1} cm^{-1}) and **F2** (418 nm, 23,695 M^{-1} cm^{-1}), the maximum absorption of **F3** (441 nm, 26,016 M^{-1} cm^{-1}) was slightly distant. Noticeably, the molar extinction coefficients of the three dyes were higher than that of the N719 dye (14.0×10^3 M^{-1} cm^{-1}) [5], thus indicating good light harvesting ability.

3.3. Molecular orbital calculations

The molecular geometries and electron distributions of **F1**, **F2**, and **F3** were obtained using the density function theory calculations with Gaussian 03 program. The calculations were performed with the B3LYP exchange correlation that is functional under 6-31G (d) basis. Results are shown in Fig. 3. The electron distribution before light irradiation locates mainly on the donor units while moving to the acceptor units close to the anchoring groups after light irradiation. This distribution favors the electron injection from the dye molecules to the conduction band edge of TiO_2.

3.4. Electrochemical properties

The redox behavior of the **F1**, **F2**, and **F3** dyes was studied by cyclic voltammetry (Fig. 4) to investigate the ability of electron transfer from the excited dye molecules to the conductive band of TiO_2. The cyclic voltammograms of **these** dyes were measured in a solution of 0.1 M *n*-Bu_4NPF_6 in CH_2Cl_2. A three-electrode cell containing a Pt-coil working electrode, a Pt wire counter electrode, and a Ag/AgCl reference electrode was employed. The ferrocene/ferricenium redox couple was used as an internal reference. The examined highest occupied molecular orbital (HOMO) levels and the lowest unoccupied molecular orbital (LUMO) levels were collected, as shown in Table 1. HOMO values (0.93 V–0.97 V vs. NHE) were more positive than the I^-/I_3^- redox couple (0.4 V vs. NHE), thus suggesting that the oxidized dyes can thermodynamically accept electrons from I^- ion in iodide/triiodide electrolyte for regeneration. Electron injection from the excited sensitizers to the conduction band of TiO_2 should be energetically favorable because of the more negative LUMO values (−1.41 V to −1.51 V vs. NHE) compared with the conduction band edge energy level of the TiO_2 electrode (at approximately −0.5 V vs. NHE) [42]. Table 1 shows that the introduction of the phenyl and *n*-hexyl groups to fluorine can change the HOMO–LUMO energy gaps of the dyes narrowly. These results clearly demonstrate that these dyes are potentially efficient dyes for DSSCs.

3.5. Photovoltaic performance

The action spectrum, or the IPCE as a function of wavelength, was measured to evaluate the photoresponse of the photoelectrode

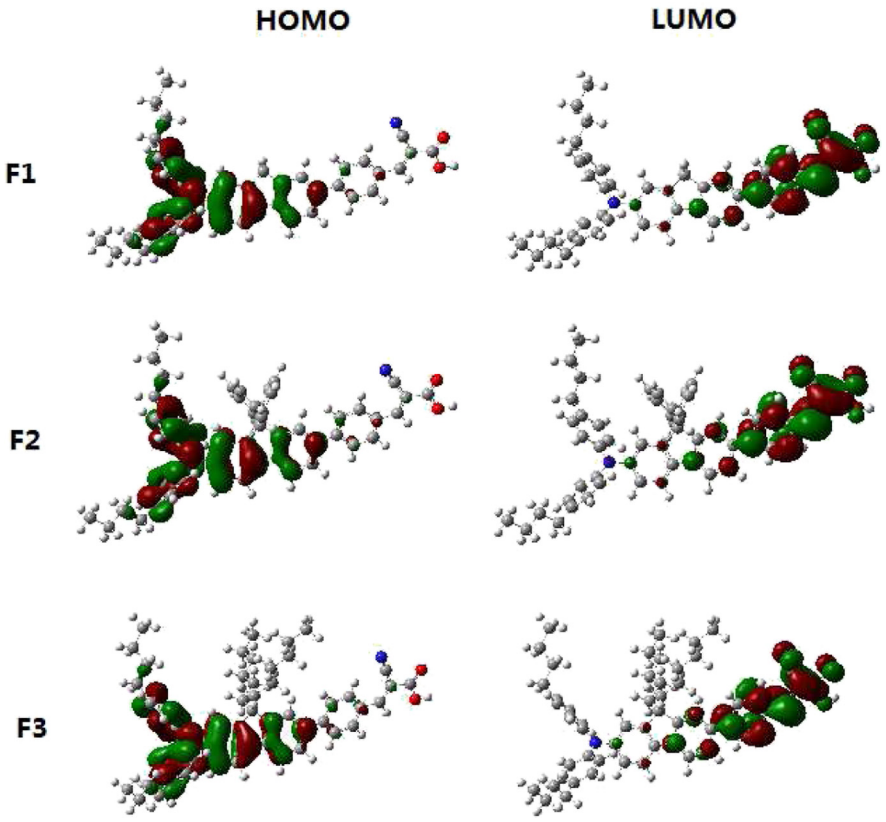

Fig. 3. Frontier HOMO and LUMO orbitals of **F1, F2,** and **F3** dyes.

in the whole spectral region. **F1**, **F2**, and **F3** sensitizers were used to manufacture solar cell devices. Fig. 5 shows the IPCE obtained with 0.06 M LiI, 0.03 M I_2, 0.1 M guanidinium thiocyanate, 0.6 M PMII, and 0.5 M *tert*-butyl-pyridine in acetonitrile as redox electrolyte. The three dyes can efficiently convert visible light into photocurrent in the region of 300 nm–600 nm. A solar cell based on **F3** showed the highest IPCE value of 75% at 490 nm. In addition, the cell exhibited a broad IPCE spectrum with IPCE values (>70%) ranging from 390 nm to 520 nm. However, the IPCE spectra of **F2** and **F1** were slightly low, with a maximum IPCE of 68% at 445 nm and 69% at 450 nm, respectively.

Fig. 6 shows the current–voltage curves of the DSSCs based on the **F1**, **F2**, and **F3** dyes under standard global AM 1.5 G solar irradiation, and the results are shown in Table 2. The DSSCs based on the **F3** dye showed the best performance, with a short-circuit photocurrent density of 9.69 mA cm^{-2}, an open-circuit voltage of 0.77 V, and a fill factor of 0.70, thereby yielding an overall conversion efficiency (η) of 5.15%. For a fair comparison, the N719-

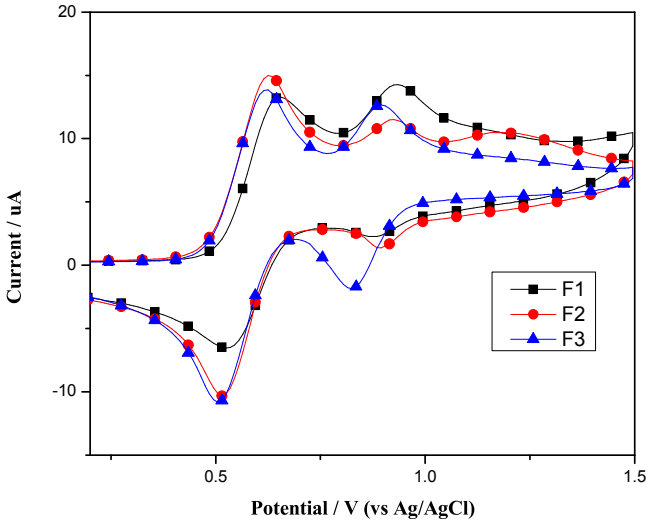

Fig. 4. Cyclic voltammogram of **F1, F2,** and **F3** in CH_2Cl_2.

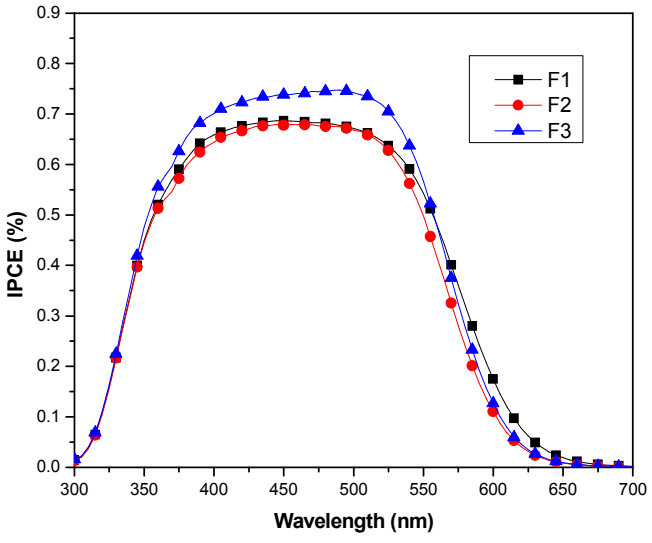

Fig. 5. IPCE spectra for DSSCs based on the as-synthesized dyes.

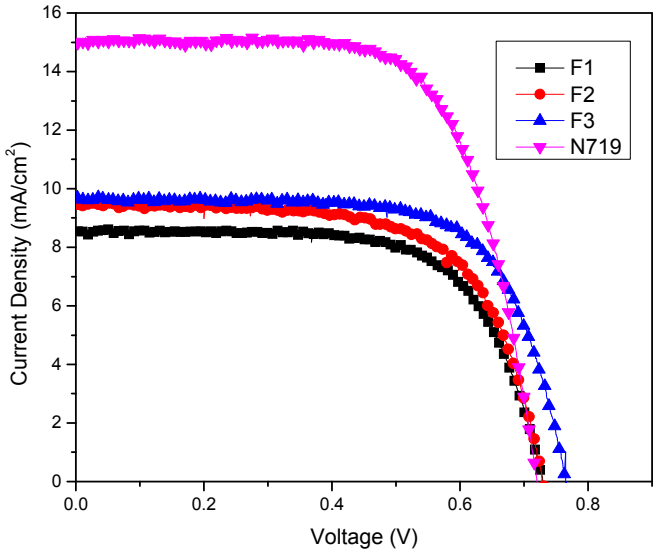

Fig. 6. Current - potential (*J*–*V*) curve for the DSSCs based on **F1**, **F2** and **F3**.

sensitized TiO_2 solar cell showed an efficiency of 7.46%, with a J_{SC} of 15.04 mA cm^{-2}, a V_{OC} of 0.72 V, and a fill factor of 0.69. The conversion efficiency of **F3** reached 70% of the N719 cell efficiency. Compared with the **F1**-based cell, the **F2**-based cell showed a lower J_{SC} value. This result indicates that the phenyl substituent can serve as a π to aggregate with the π-spacer of the **F2** dye. The **F3**-based cell gives a higher J_{SC} value than the **F1**-based cell, thereby reflecting its better ability to avoid π–π aggregation as a result of the *n*-hexyl as a substituent [43].

Chenodeoxycholic acid (CDCA) is used as coadsorbent to dissociate the π-stacked dye aggregates and to improve the electron injection yield, thus affording a high J_{SC} value (Table 2). For the DSSCs sensitized by the dyes, the J_{SC} values of the **F1** and **F2** dyes with CDCA increased by 0.38 and 0.11 mA cm^{-2}, respectively. However, the J_{SC} values were reduced from 0.52 mA cm^{-2} to 9.17 mA cm^{-2} for the **F3** dye because of the decrease in the loading dyes. The results confirm again that the use of the *n*-hexyl chain can avoid the π–π aggregation of the dyes and consequently achieve a high short-circuit current density.

4. Conclusions

In summary, three new organic sensitizers (**F1**, **F2**, and **F3**) containing different groups (hydrogen, phenyl, and *n*-hexyl) substituted on fluorene moieties were designed and synthesized for DSSCs. The introduction of phenyl-substituted fluorene moiety (**F2**) increased the π–π aggregation, thus leading to low short-circuit current density. The use of *n*-hexyl-substituted fluorene moiety can avoid the π–π aggregation of the dyes and consequently achieve a high conversion efficiency (5.15%). Our results indicate that the alkyl group is better than the aryl group in avoiding the π–π aggregation. The detailed investigation into the effect of the substitution on π-spacer with other bulky groups is ongoing in our laboratory.

Table 2
Photovoltaic performance of DSSCs sensitized with the as-synthesized dyes compared with the N719 dye.[a]

Dye	CDCA	J_{SC}/mA cm^{-2}	V_{oc}/mV	ff	η/%
F1	0 mM	9.40	0.73	0.67	4.62
	0.8 mM	9.78	0.75	0.69	5.11
F2	0 mM	8.51	0.73	0.69	4.26
	0.8 mM	8.62	0.74	0.71	4.55
F3	0 mM	9.69	0.77	0.70	5.15
	0.8 mM	9.17	0.72	0.66	4.39
N719	0 mM	15.04	0.72	0.69	7.46

[a] The DSSCs had an active area of ~0.16 cm^2 and used an electrolyte composed of 0.06 M LiI, 0.03 M I_2, 0.1 M guanidinium thiocyanate, 0.6 M 1-propyl-3-methylimidazolium iodide (PMII), and 0.5 M *tert*-butyl-pyridine in acetonitrile.

Acknowledgments

We are grateful to the National Natural Science Foundation of China (No. 21002010 and 21273026) for their financial support. This work was also supported by the Fundamental Research Funds for the Central Universities (DUT12LK44).

References

[1] O'Regan B, Grätzel M. A low-cost, high-efficiency solar cell based on dye-sensitized colloidal TiO_2 films. Nature 1991;353:737–9.
[2] Grätzel M. Dye-sensitized solar cells. J Photochem Photobiol C 2003;4:145–53.
[3] Grätzel M. Conversion of sunlight to electric power by nanocrystalline dye-sensitized solar cells. J Photochem Photobiol A 2004;164:3–14.
[4] Nazeeruddin MK, Kay A, Rodicio I, Humphry-Baker R, Müller E, Liska P, et al. Conversion of light to electricity by *cis*-X_2bis(2,2'-bipyridyl-4,4'-dicarboxylate) ruthenium(II) charge-transfer sensitizers (X = Cl^-, Br^-, I^-, CN^- and SCN^-) on nanocrystalline TiO_2 electrodes. J Am Chem Soc 1993;115:6382–90.
[5] Nazeeruddin MK, Zakeeruddin SM, Humphry-Baker R, Jirousek M, Liska P, Vlachopoulos N, et al. Acid-base equilibria of (2,2'-bipyridyl-4,4'-dicarboxylic acid) ruthenium(II) complexes and the effect of protonation on charge-transfer sensitization of nanocrystalline titania. Inorg Chem 1999;38:6298–305.
[6] Nazeeruddin MK, Péchy P, Renouard T, Zakeeruddin SM, Humphry-Baker R, Comte P, et al. Engineering of efficient panchromatic sensitizers for nanocrystalline TiO_2-based solar cells. J Am Chem Soc 2001;123:1613–24.
[7] Ning ZJ, Zhang Q, Wu WJ, Pei HC, Liu B, Tian H. Starburst triarylamine based dyes for efficient dye-sensitized solar cells. J Org Chem 2008;73:3791–7.
[8] Wiberg J, Marinado T, Hagberg DP, Sun LC, Hagfeldt A, Albinsson B. Distance and driving force dependencies of electron injection and recombination dynamics in organic dye-sensitized solar cells. J Phys Chem B 2010;114:14358–63.
[9] Chang DW, Lee HJ, Kim JH, Park SY, Park SM, Dai LM, et al. Novel quinoxaline-based organic sensitizers for dye-sensitized solar cells. Org Lett 2011;13:3880–3.
[10] Gao FF, Wang Y, Shi D, Zhang J, Wang MK, Jing XY, et al. Enhance the optical absorptivity of nanocrystalline TiO_2 film with high molar extinction coefficient ruthenium sensitizers for high performance dye-sensitized solar cells. J Am Chem Soc 2008;130:10720–8.
[11] Späth M, Sommeling PM, van Roosmalen JAM, Smit HJP, van der Burg NPG, Mahieu DR, et al. Reproducible manufacturing of dye-sensitized solar cells on a semi-automated baseline. Prog Photovolt 2003;11:207–20.
[12] Hwang S, Lee JH, Park C, Lee H, Kim C, Park C, et al. A highly efficient organic sensitizer for dye-sensitized solar cells. Chem Commun 2007:4887–9.
[13] Kitamura T, Ikeda M, Shigaki K, Inoue T, Anderson NA, Ai X, et al. Phenyl-conjugated oligoene sensitizers for TiO_2 solar cells. Chem Mater 2004;16:1806–12.
[14] Chen KF, Hsu YC, Wu QY, Yeh MCP, Sun SS. Structurally simple dipolar organic dyes featuring 1,3-cyclohexadiene conjugated unit for dye-sensitized solar cells. Org Lett 2009;11:377–80.
[15] Yang CH, Chen HL, Chuang YY, Wu CG, Chen CP, Liao SH, et al. Characteristics of triphenylamine-based dyes with multiple acceptors in application of dye-sensitized solar cells. J Power Sources 2009;188:627–34.
[16] Liang M, Xu W, Cai FS, Chen PQ, Peng B, Chen J, et al. New triphenylamine-based organic dyes for efficient dye-sensitized solar cells. J Phys Chem C 2007;111:4465–72.
[17] Kim C, Choi H, Kim S, Baik C, Song K, Kang MS, et al. Molecular engineering of organic sensitizers containing *p*-phenylene vinylene unit for dye-sensitized solar cells. J Org Chem 2008;73:7072–9.
[18] Xu W, Peng B, Chen J, Liang M, Cai FS. New triphenylamine-based dyes for dye-sensitized solar cells. J Phys Chem C 2008;112:874–80.
[19] Liu WH, Wu IC, Lai CH, Lai CH, Chou PT, Li YT, et al. Simple organic molecules bearing a 3,4-ethylenedioxythiophene linker for efficient dye-sensitized solar cells. Chem Commun 2008:5152–4.
[20] Hagberg DP, Marinado T, Karlsson KM, Nonomura K, Qin P, Boschloo G, et al. Tuning the HOMO and LUMO energy levels of organic chromophores for dye sensitized solar cells. J Org Chem 2007;72:9550–6.
[21] Shi D, Cao YM, Pootrakulchote N, Yi ZH, Xu MF, Zakeeruddin SM, et al. New organic sensitizer for stable dye-sensitized solar cells with solvent-free ionic liquid electrolytes. J Phys Chem C 2008;112:17478–85.

[22] Yum JH, Hagberg DP, Moon SJ, Karlsson KM, Marinado T, Sun LC, et al. A light-resistant organic sensitizer for solar-cell applications. Angew Chem Int Ed 2009;48:1576–80.
[23] Li G, Jiang KJ, Li YF, Li SL, Yang LM. Efficient structural modification of triphenylamine-based organic dyes for dye-sensitized solar cells. J Phys Chem C 2008;112:11591–9.
[24] Xu MF, Li RZ, Pootrakulchote N, Shi D, Guo J, Yi ZH, et al. Energy-level and molecular engineering of organic D-π-A sensitizers in dye-sensitized solar cells. J Phys Chem C 2008;112:19770–6.
[25] Wang MK, Xu MF, Shi D, Li RZ, Gao FF, Zhang GL, et al. High-performance liquid and solid dye-sensitized solar cells based on a novel metal-free organic sensitizer. Adv Mater 2008;20:4460–3.
[26] Zhang GL, Bai Y, Li RZ, Shi D, Wenger S, Zakeeruddin SM, et al. Employ a bisthienothiophene linker to construct an organic chromophore for efficient and stable dye-sensitized solar cells. Energy Environ Sci 2009;2:92–5.
[27] Zhang GL, Bala H, Cheng YM, Shi D, Lv XJ, Yu QJ, et al. High efficiency and stable dye-sensitized solar cells with an organic chromophore featuring a binary π-conjugated spacer. Chem Commun 2009;2:198–200.
[28] Qin H, Wenger S, Xu M, Gao F, Jing X, Wang P, et al. An organic sensitizer with a fused dithienothiophene unit for efficient and stable dye-sensitized solar cells. J Am Chem Soc 2008;130:9202–3.
[29] Tian HN, Yang XC, Chen RK, Zhang R, Hagfeldt A, Sun LC. Effect of different dye baths and dye-structures on the performance of dye-sensitized solar cells based on triphenylamine dyes. J Phys Chem C 2008;112:11023–33.
[30] Choi H, Lee JK, Song K, Kang SO, Ko J. Novel organic dyes containing bis-dimethylfluorenyl amino benzo[*b*]thiophene for highly efficient dye-sensitized solar cell. Tetrahedron 2007;63:3115–21.
[31] Choi H, Baik C, Kang SO, Ko J, Kang MS, Nazeeruddin MK, et al. Highly efficient and thermally stable organic sensitizers for solvent-free dye-sensitized solar cells. Angew Chem Int Ed 2008;47:327–30.
[32] Velusamy M, Thomas KRJ, Lin JT, Hsu YC, Ho KC. Organic dyes incorporating low-band-gap chromophores for dye-sensitized solar cells. Org Lett 2005;7:1899–902.
[33] Lee DH, Lee MJ, Song HM, Song BJ, Seo KD, Pastore M, et al. Organic dyes incorporating low-band-gap chromophores based on π-extended benzothiadiazole for dye-sensitized solar cells. Dyes Pigments 2011;91:192–8.
[34] Seo KD, Choi IT, Park YG, Kang S, Lee JY, Kim HK. Novel D-A-π-A coumarin dyes containing low band-gap chromophores for dye-sensitised solar cells. Dyes Pigments 2012;94:469–74.
[35] Haid S, Marszalek M, Mishra A, Wielopolski M, Teuscher J, Moser J, et al. Significant improvement of dye-sensitized solar cell performance by small structural modification in π-conjugated donor–acceptor dyes. Adv Funct Mater 2012;22:1291–302.
[36] Akhtaruzzaman Md, Seya Y, Asao N, Islam A, Kwon E, EI-Shafei A, et al. Donor-acceptor dyes incorporating a stable dibenzosilole π-conjugated spacer for dye-sensitized solar cells. J Mater Chem 2012;22:10771–8.
[37] Wu YZ, Zhang X, Li WQ, Wang ZS, Tian H, Zhu WH. Hexylthiophene-featured D–A–π–A structural indoline chromophores for coadsorbent-free and panchromatic dye-sensitized solar sells. Adv Energy Mater 2012;2:149–56.
[38] Huang WY, Huang SY. Sterically encumbered fluorene-based poly(arylene ether)s containing spiro-annulated substituents on the main chain. Macromolecules 2010;43:10355–65.
[39] Saikia G, Iyer PK. Facile C-H alkylation in water: enabling defect-free materials for optoelectronic devices. J Org Chem 2010;75:2714–7.
[40] Frisch MJ, Trucks GW, Schlegel HB, Scuseria GE, Robb MA, Cheeseman JR, et al. Gaussian 03, revision C.02. Wallingford, CT: Gaussian Inc.; 2004.
[41] Guo W, Shen YH, Wu LQ, Gao YR, Ma TL. Effect of N dopant amount on the performance of dye-sensitized solar cells based on N-doped TiO_2 electrodes. J Phys Chem C 2011;115:21494–9.
[42] Hao Y, Yang XC, Cong JY, Tian HN, Hagfeldt A, Sun LC. Efficient near infrared D–π–A sensitizers with lateral anchoring group for dye-sensitized solar cells. Chem Commun 2009:4031–3.
[43] Koumura N, Wang ZS, Mori S, Miyashita M, Suzuli E, Hara K. Alkyl-functionalized organic dyes for efficient molecular photovoltaics. J Am Chem Soc 2006;128:14256–7.